Catalysis Today 419 (2023) 114150

Contents lists available at ScienceDirect

Catalysis Today

journal homepage: www.elsevier.com/locate/cattod

Enhanced solar driven photocatalytic removal of antibiotics from aquaculture effluents by TiO_2/carbon quantum dot composites

Valentina Silva [a], Joana F.A. Fernandes [b], Maria Clara Tomás [b], Carla Patrícia Silva [a], Vânia Calisto [a,*], Marta Otero [c], Diana L.D. Lima [a]

[a] CESAM, Department of Chemistry, University of Aveiro, Campus de Santiago, 3810-193 Aveiro, Portugal
[b] Department of Chemistry, University of Aveiro, Campus de Santiago, 3810-193 Aveiro, Portugal
[c] Departamento de Química y Física Aplicadas, Universidad de León, Campus de Vegazana, 24071 León, Spain

ARTICLE INFO

Keywords:
Sulfadiazine
Sulfamethoxazole
Trimethoprim
Aquaculture effluents treatment
Visible-light photocatalysis

ABSTRACT

Aquaculture exploitation is associated with the consumption of antibiotics, such as sulfadiazine (SDZ), sulfamethoxazole (SMX) and trimethoprim (TMP), the latter two being also vastly used to treat bacterial infections in humans. Consequently, and given that aquaculture wastewater treatments are not actually designed for the removal of antibiotics, they are ubiquitous in aquaculture effluents, which sets the risk of bacterial resistance. To face the need for an efficient and sustainable treatment to remove these antibiotics from the referred effluents, carbon quantum dots (CQDs) were produced, incorporated into titanium dioxide (TiO_2), and evaluated for solar driven photodegradation of SDZ, SMX and TMP. Eleven different materials were synthesized and tested for their photocatalytic activity in phosphate buffer solution (PBS) and synthetic sea salts (SSS), used as synthetic matrices to simulate fresh and brackish water, respectively. Upon selection of the most efficient photocatalyst for each antibiotic and matrix, kinetic results demonstrated that its use allowed for remarkable reductions of SDZ, SMX and TMP half-life times ($t_{1/2}$) in both matrices (between 19 and 68 times). Therefore, the application of the here synthesized photocatalysts for the advanced treatment of aquaculture effluents is promising, allowing for a green solar driven removal of antibiotics.

1. Introduction

Antibiotics have been extremely important for the development of society, namely by the treatment and prevention of bacterial infections in human and veterinary medicine. Excretion of the original compound or a metabolized form, together with the inadequate disposal of unused pharmaceuticals, are important sources of antibiotics in water systems, promoting the presence of this type of compounds in the environment [1]. Although sources from human consumption have received more attention, antibiotics are also highly used in concentrated animal feeding operations, and, in the particular case of aquaculture, a significant part of the administered doses may not be eaten or absorbed by fish and/or not fully metabolized, so antibiotics may be released in the original form [2–4]. Aquacultures are not equipped with methods to efficiently remove antibiotics from effluents (either from fresh, brackish, or salted water). Therefore, they are directly discharged into the aquatic

Abbreviations: **CQDs**, Carbon Quantum Dots; **CQDs-CA**, Carbon Quantum Dots produced with citric acid; **CQDs-CAC**, Carbon Quantum Dots produced with citric acid and calcinated; **CQDs-CAU**, Carbon Quantum Dots produced with citric acid and urea; **CQDs-CAUC**, Carbon Quantum Dots produced with citric acid and urea and calcinated; **PBS**, phosphate buffer solution; **SSS**, synthetic sea salts; **TiO_2C**, calcinated TiO_2; **TiO_2/CQDs**, composites of Titanium Dioxide and Carbon Quantum Dots; **TiO_2/CQDs-CA 4% *w/w***, composites of Titanium Dioxide with 4% (*w/w*) of Carbon Quantum Dots produced with citric acid; **TiO_2/CQDs-CA 5% *w/w***, composites of Titanium Dioxide with 5% (*w/w*) of Carbon Quantum Dots produced with citric acid; **TiO_2/CQDs-CA 6% *w/w***, composites of Titanium Dioxide with 6% (*w/w*) of Carbon Quantum Dots produced with citric acid; **TiO_2/CQDs-CA 8% *w/w***, composites of Titanium Dioxide with 8% (*w/w*) of Carbon Quantum Dots produced with citric acid; **TiO_2/CQDs-CAU 4% *w/w***, composites of Titanium Dioxide with 4% (*w/w*) of Carbon Quantum Dots produced with citric acid and urea; **TiO_2/CQDs-CAU 5% *w/w***, composites of Titanium Dioxide with 5% (*w/w*) of Carbon Quantum Dots produced with citric acid and urea; **TiO_2/CQDs-CAU 6% *w/w***, composites of Titanium Dioxide with 6% (*w/w*) of Carbon Quantum Dots produced with citric acid and urea; **TiO_2/CQDs-CAU 8% *w/w***, composites of Titanium Dioxide with 8% (*w/w*) of Carbon Quantum Dots produced with citric acid and urea.

* Corresponding author.
E-mail address: vania.calisto@ua.pt (V. Calisto).

https://doi.org/10.1016/j.cattod.2023.114150
Received 19 December 2022; Received in revised form 17 March 2023; Accepted 4 April 2023
Available online 6 April 2023

environment, where they may persist, altering the water quality and affecting the aquatic organisms [3,4].

The antibiotics sulfadiazine (SDZ) and sulfamethoxazole (SMX), which belong to the sulfonamides class, and trimethoprim (TMP), which is a diaminopyrimidine, are some of the most frequently used antibiotics in aquaculture [5] and have been detected in surface waters [6,7]. Furthermore, both SMX and TMP are also applied for the treatment of human bacterial diseases, being part of the World Health Organization's Model List of Essential Medicines (22nd list) [8]. The presence of antibiotics in the environment can be dangerous to aquatic organisms and also to humans [9,10], and may even induce antibiotic-resistant genes leading to the increase of antimicrobial resistance, which is considered one of the biggest public health threats of the 21st century [11,12]. Furthermore, under the European Union Water Framework Directive (Directive 2000/60/EC), SMX and TMP, which were already considered in the 3rd watch list (Decision 2020/1161), were also included in the 4th (and last) watch list (Decision 2022/1307).

So far, different processes have been applied in the removal of antibiotics from water, including adsorption, advanced oxidation processes, biological treatment, and photocatalytic degradation [13–17]. Among them, photodegradation has been considered an effective approach to remove or, at least, reduce the concentration of antibiotics in the environment and solar driven photolysis represents an unexpensive, green and sustainable solution [18,19]. Furthermore, phototreatments may allow for the replacement of pre-existent wastewater treatment processes that are considered either expensive, such as UV oxidation, or harmful, such as ozonation (due to the formation of toxic by-products, like bromoform ($CHBr_3$) and bromate (BrO_3^-), from the reaction between ozone and natural constituents of salty water) [20].

Many researchers have studied the application of photocatalysis for the removal of antibiotics from water [21,22], including the use of titanium dioxide (TiO_2) [23,24]. Titanium dioxide (TiO_2) is a semiconductor thoroughly studied as heterogeneous photocatalyst for environmental applications [23] due to its low price, commercial availability, photochemical stability, and absence of toxicity [25,26]. However, there are some drawbacks concerning TiO_2, including low utilization of sunlight due to the high band gap energy (~3.2 eV) and rapid recombination of photogenerated electrons and holes [27,28]. In order to overcome these issues, doping of TiO_2 using different dopants has shown good results, especially with non-metals, such as carbon quantum dots (CQDs) [29], since they avoid the possible photo-corrosion dangers associated to metals [30]. CQDs are fluorescent carbon-based nanoparticles with a spherical or quasi-spherical shape that are inexpensive and have excellent optical properties, low toxicity, high chemical stability and efficient electron transfer properties, having been successfully used to bridge TiO_2 limitations and promote its photocatalytic activity [31]. As reported by Yu et al. [32], semiconductor/CQDs hybrid photocatalysts exhibit outstanding optical properties and photogenerated carriers transfer characteristics. Additionally, the introduction of CQDs not only broadens the photo absorption region and suppresses the combination of photogenerated electrons and holes of TiO_2, but also facilitates the consumption of holes and promotes redox reaction [33].

TiO_2/CQDs composites were first evaluated for the photocatalytic removal of antibiotics from water by Chen et al. [34]. These authors used a hydrothermal-calcination method to functionalize TiO_2 with CQDs (1.0%, 5.0%, 10.0% and 20% (*w/w*) CQDs) and the composite with 5% (*w/w*) CQDs, which was selected as the most efficient, provided 2.3 times faster gemfibrozil photodegradation than TiO_2 under simulated sunlight. Then, Sharma et al. [35] synthesized a TiO_2/CQDs photocatalyst that provided nearly complete removal of levofloxacin within 90 min of sunlight irradiation (in comparison with 66.5% with bare TiO_2). Testing different CQDs loadings, namely 2.0%, 4.0%, 6.0% and 8.0% (*w/w*), Zeng et al. [36] produced TiO_2/CQDs for the photocatalytic removal of ciprofloxacin. Among them, that with 6.0% (*w/w*) CQDs achieved the maximum antibiotic removal (≈ 98%) after sunlight irradiation during 30 min (in comparison with 64% by pristine TiO_2). Wang et al. [37] also tested different CQDs loadings (1.0%, 3.0%, 5.0% and 7.0% (*w/w*)) in TiO_2/CQDs composites, with the most efficient (5.0% (*w/w*) CQDs) allowing for 81% degradation of tetracycline after 10 min irradiation, in comparison with 25% by TiO_2. More recently, TiO_2/CQDs composites were tested as photocatalysts for aquaculture antibiotics [38,39]. Louros et al. [38] showed that the composites exhibited a more remarkable photocatalytic performance than pristine TiO_2 for either SDZ or oxolinic acid, but a much poorer performance was observed for the latter, especially in simulated marine aquaculture effluents. Thus, Silva et al. [39] tested different CQDs and their TiO_2 composites with different CQDs loadings (4.0%, 5.0%, 6.0% and 8.0% (*w/w*)) with the aim of removing oxolinic acid even from saline water matrices (after 1 h of irradiation, the most efficient composite provided a 75% removal in comparison with 17% by TiO_2).

In this work, TiO_2/CQDs composites were tested for the photodegradation of the most used antibiotics in aquaculture, namely SDZ, SMX and TMP, under simulated solar irradiation. The evaluation was performed in two different aqueous matrices (phosphate buffer solution (PBS) and synthetic sea salts (SSS)) simulating fresh and brackish water and the photocatalytic conditions were optimized to develop a good basis for TiO_2/CQDs application for antibiotic removal from aquaculture effluents.

2. Materials and methods

2.1. Chemicals and solutions

SDZ (> 98%) and SMX (> 98%) were provided from TCI Chemicals, while TMP (> 98%) was from Sigma-Aldrich. Ultrapure water was obtained using a Purelab Flex 4 purification water system from Elga (Veolia). A 0.1 mol L^{-1} phosphate buffer stock solution (1 L), pH 8.6, was prepared using 0.6 g of sodium dihydrogen phosphate dihydrate (Fluka, Biochemika, ≥ 99.5%) and 17.1 g of di-sodium hydrogen phosphate dihydrate (Fluka, Biochemika, ≥ 99%), which was then diluted to 0.001 mol L^{-1} in ultrapure water to obtain PBS used in this work. Red Sea Salt (Red Sea Europe) was dissolved in ultrapure water at a concentration of 30 g L^{-1} to prepare SSS. The antibiotic stock solutions were prepared by dissolving 10 mg of the corresponding reagent in PBS or in SSS (details are given within Section 2.3.) and left to dissolve overnight. Citric acid monohydrated (Pronalab, ≥ 99.5%), urea (Panreac, ≥ 99.0%), sodium hydroxide (pellets, Akzo Nobel), hydrochloric acid (NormaPur, 37%) and ultrapure water were used for the synthesis of CQDs. For the incorporation of CQDs in TiO_2, titanium (IV) oxide (aeroxide P25, Acros Organic) and ethanol absolute anhydrous (Carlo Erba) were used. For high-performance liquid chromatography with a UV–visible detector (HPLC-UV) analysis, methanol (Fisher Scientific, HPLC grade) and formic acid (Sigma-Aldrich, > 98%) were used.

2.2. Carbon quantum dots synthesis and incorporation of CQDs into TiO_2

Two types of CQDs were used in this work, namely CQDs-citric acid (CQDs-CA) and CQDs-citric acid and urea (CQDs-CAU) so to compare their photocatalytic performance. Citric acid is one of the most used carbon sources for the synthesis of CQDs aimed at producing TiO_2/CQDs for pharmaceuticals photocatalytic removal from water [31]. On the other hand, urea has been successfully used together with citric acid as nitrogen source for the synthesis of N-doped CQDs by hydrothermal treatment [40]. N-doping has been shown to provide excellent photocatalytic properties to CQDs [41]. The nitrogen bond to carbon can enhance the photoluminescence emission by inducing an upward shift in the Fermi level [42] and N-doped CQDs are known to have increased fluorescence quantum yield in comparison with non-doped CQDs [40]. It is believed that electrons are injected from the N-dopant into CQDs, changing their local electronic structure, increasing their capacitance, and favouring binding with ions [43,44].

Details on the synthesis of CQDs-CA, CQDs-CAU and TiO_2/CQDs composites were given in Silva et al. [39]. Briefly, CQDs-CA were synthesized by the decomposition of 40 g citric acid in an electric furnace (Memmert) for 40 h at 180 ℃. The resulting brown gelatinous matter was dissolved in a 5 mol L^{-1} NaOH solution, and the pH was adjusted to 7 with 2 mol L^{-1} HCl. Finally, the CQDs were freeze-dried to obtain the CQDs powder. Meanwhile, CQDs-CAU were produced by a hydrothermal method as follows: citric acid (3.0 g) and urea (3.0 g) were mixed with 10 mL of ultrapure water and placed into a 50 mL autoclave for 5 h at 180 ℃; then, the large particles were removed by centrifugation at 5000 *rpm* for 30 min, using a centrifuge (SIGMA 4–10) and the remaining solution was freeze-dried to obtain the CQDs-CAU. The production yield, as the amount of CQDs obtained from the used precursor (s) (% (*w/w*)), was 51% for CQDs-CA and 37% for CQDs-CAU.

After CQDs synthesis, TiO_2/CQDs with different mass percentages of CQDs, namely 4%, 5%, 6% and 8% (*w/w*), which choice was based on previously reported values for TiO_2/CQDs aimed at antibiotics photocatalysis (as referred in the introduction section), were obtained through hydrothermal calcination. For such a purpose, 1.00 g of TiO_2 powder was dispersed in 30 mL of ethanol in an alumina crucible and the corresponding volume of a solution of 50 g L^{-1} of CQDs (CQDs-CA or CQDs-CAU) was added to obtain TiO_2/CQDs composites with 4%, 5%, 6% and 8% CQDs (*w/w*). Finally, the composites were dried at 75 °C and then heated at 10 °C min^{-1} in a muffle furnace (Nüve, model MF110) until 300 °C, which was then maintained for 3 h. The obtained composites were labelled as TiO_2/CQDs, followed by the CQDs precursor(s) abbreviation (CA or CAU) and the CQDs mass percentage (% (*w/w*)) (e.g., TiO_2/CQDs-CAU 4% (*w/w*)). A batch of each type of CQDs and a batch of TiO_2 was individually subjected to the calcination process to obtain calcinated CQDs-CA (CQDs-CAC), calcinated CQDs-CAU (CQDs-CAUC) and calcinated TiO_2 (TiO_2C). A total of eleven different materials were produced (their characterization is detailed elsewhere [39]).

2.3. Water matrices

The water matrix can influence the photodegradation behaviour of organic compounds, including antibiotics [17,19,45]. Since SDZ, SMX and TMP may be used in both fresh and saltwater aquaculture, PBS and SSS, which preparation was above described (Section 2.1), were respectively used as matrices simulating fresh and brackish water. The water matrices were characterized by measuring the pH, salinity, and conductivity. For PBS, these parameters were respectively measured as 8.6, 0.0 and 0.2 mS cm^{-1}. Meanwhile, for SSS, they were 8.6, 25.8 and 40.4 mS cm^{-1}, respectively.

2.4. Photodegradation apparatus

Irradiation experiments were carried out in a solar radiation simulator Solarbox 1500 (Co.fo.me.gra, Italy) equipped with a xenon arc lamp (1500 W) and UV filters that limit the transmission of light below 290 nm. All experiments were performed with a constant irradiation of 55 W m^{-2} (290–400 nm), which corresponds to 550 W m^{-2} in the spectral range, according to the manufacturer. The level of irradiance and temperature was monitored by a multimeter (Co.fo.me.gra, Italy) equipped with a UV 290–400 nm band sensor and a black standard temperature sensor. A parabolic reflection system was used to ensure irradiation uniformity in the chamber, which was kept refrigerated by an air-cooling system.

2.5. Photocatalytic experiments: photocatalyst selection, dosage evaluation and kinetics

The produced materials were tested for the photocatalysis of each antibiotic in each water matrix (PBS or SSS). For that, the corresponding mass of each photocatalyst was weighted into the quartz tubes (internal diameter × height = 1.8 × 20 cm), in triplicate, and, after pouring the antibiotic aqueous solution (20 mL, 10 mg L^{-1}), the tubes were manually agitated for homogenization. Then, tubes were placed inside the solar radiation simulator, where they were maintained under irradiation during a pre-set time. The concentrations of photocatalyst used in the experiments and the irradiation times can be found in Table S1, in SM. For comparison, photolysis experiments were performed using tubes with the antibiotic solution (20 mL, 10 mg L^{-1}), without any photocatalyst, and irradiated during the same time. Also, dark controls were run under identical conditions as photocatalysis and photodegradation experiments except for irradiation (quartz tubes covered by aluminium foil) and maintained inside the solar simulator during the same time as the irradiated solutions. After the corresponding irradiation time, aliquots (1.0 mL) were collected from the replicated irradiated solutions and dark controls, filtered using a syringe filter of PVDF 0.22 μm (Whatman), stored in the dark at 4 ℃ and analysed within 24 h for the antibiotic concentration (details are given in Section 2.6. Chromatographic analyses). The percentage of antibiotic degradation, in presence and absence of each photocatalyst, was determined by comparison of the concentration of antibiotic in irradiated solutions (C) with that in the respective dark controls (C_0). Considering the calibration curves and limits of detection of the chromatographic methodology here used (see Section 2.6. Chromatographic analysis), the antibiotics initial concentration (10 mg L^{-1}) was selected to allow photodegradation monitoring until a 99% threshold for the three of them. Regarding the photocatalyst dosages and irradiation times applied in these and subsequent experiments, they were set as a compromise for each antibiotic and matrix so to ensure significant differences between C and C_0, while avoiding multiple C values lower than the corresponding limit of detection (LOD, as described in Section 2.6. Chromatographic analysis), which would inhibit the comparison of photocatalysts' performance.

One-way ANOVA was used to compare the photocatalytic efficiencies of the synthesized materials in the removal of SDZ, SMX and TMP. Photocatalysts with significantly larger efficiencies ($p > 0.05$) were selected for further studies, where their dosages were optimized. For this purpose, photodegradation experiments were carried out as previously described but testing different concentrations of each of the selected photocatalysts. The photocatalyst concentrations tested for each antibiotic and matrix varied between 100 and 1000 mg L^{-1}, depending on the antibiotic under study (details can be found in Table S2, in SM). In what concerns irradiation times, 0.3 h was used for SDZ in PBS and SSS, while for SMX 0.25 and 0.5 h were used for PBS and SSS, respectively. For TMP in PBS, 0.2 h was initially used, but an irradiation time of 0.1 h was then used to test higher photocatalyst concentrations; meanwhile, for TMP in SSS, the irradiation time was 0.25 h. Again, photocatalysts' concentrations and irradiation times were selected as a compromise to ensure significant differences between C and C_0, while avoiding multiple C values lower than the corresponding LOD.

The most efficient TiO_2/CQDs and their dosages were used in photocatalytic experiments at increasing times (t (h)), which were carried out, either in PBS or SSS, to determine the photodegradation kinetics of SDZ, SMX and TMP in each matrix. For each antibiotic, matrix and pre-set t (h), three quartz tubes (in triplicate) were irradiated so to avoid any possible photocatalyst withdrawal during the aliquots collection throughout time. For comparison, photodegradation kinetic experiments for each antibiotic and matrix in the absence of photocatalyst were also carried out. In order to obtain the photodegradation kinetic curves, C/C_0 was determined at each t (h). GraphPad Prism 8 was used to determine the fittings of experimental data to the pseudo first-order kinetic equation $C/C_0 = e^{-kt}$, where k is the pseudo first-order degradation rate constant (h^{-1}). Also, antibiotics' half-life times ($t_{1/2}$) were calculated as $\frac{\ln(2)}{k}$.

2.6. Chromatographic analysis

Quantitative analysis of SDZ, SMX and TMP was performed using HPLC-UV. The device consisted of a Waters Alliance 2695 Separations Module equipped with a Waters 2487 Dual Absorbance detector. Separation was carried out using a 150 mm × 4.6 mm i.d. ACE® C18 column-PFP (5 μm particle size) connected to a 4.6 mm i.d. ACE® 5 C18 guard column at 25 °C. The mobile phase consisted of methanol:0.1% formic acid, 20:80 (*v/v*) at a flow rate of 0.9 mL min^{-1} for SDZ; acetonitrile:0.1% formic acid, 30:70 (*v/v*) at a flow rate of 0.8 mL min^{-1} for SMX; and acetonitrile:0.1% formic acid, 15:85 (*v/v*) at a flow rate of 0.8 mL min^{-1} for TMP. Before use, mobile phases were filtered through a 0.2 μm polyamide membrane filter (Whatman). Samples and standards were filtered by a syringe filter of PVDF 0.22 μm. An injection volume of 20 μL was used and detection was performed at 270 nm. In order to obtain the calibration curve for each antibiotic, the corresponding standard solutions, with concentrations between 0.25 and 10 mg L^{-1}, were prepared from the respective stock solutions (10 mg L^{-1}) and analysed in triplicate. The linear regression equations for SDZ, SMX and TMP were obtained and the respective LOD, in mg L^{-1}, were determined by $[LOD]=\frac{(3\times S_b)}{m}$, where S_b is the standard deviation of the *y*-interception of the slope and *m* is the slope. Calibration curves and respective LOD are presented in Table S3, in SM.

3. Results and discussion

3.1. Selection of the most efficient photocatalysts

The photodegradation results of SDZ, SMX and TMP in different matrices (PBS and SSS), in the absence and in the presence of the synthesized photocatalysts are presented in Fig. 1. It is to highlight that, for the three antibiotics, the concentration in the respective dark controls, either in PBS or SSS, was equal to C_0, which proves that the concentration decrease under irradiation was just due to photodegradation. As it may be seen in Fig. 1, different C/C_0 were observed depending on the antibiotic and the matrix. However, it must be considered that, as referred in Section 2.5., irradiation times and dosages were selected as a compromise, so comparisons are not possible at this point.

Among the here tested photocatalysts, composites obtained using CQDs-CAU were clearly more efficient than those with CQDs-CA in the photocatalytic removal of the studied antibiotics, except for SDZ in PBS. The FTIR-ATR spectra obtained for these materials (reported elsewhere [39]) evidenced the complex chemical composition of the synthesized CQDs. This complexity was especially relevant in the case of CQDs-CAU, which may be due to the incorporation of nitrogen from urea. The self-passivated nitrogen and oxygen containing functional groups on CQDs surface may be responsible for their efficient photoluminescence [46]. Also, it may be observed that TiO_2/CQDs-CAU 4% (*w/w*) was the most or among the most efficient photocatalysts for the considered antibiotics and matrices. This may be related to the fact that incorporation of CQDs at 4% (*w/w*) increased the UV–visible spectra absorption when compared with TiO_2C (reported elsewhere [39]). Still, the band gap energy of TiO_2/CQDs-CAU 4% (*w/w*) was the same as that of TiO_2C (3.2 eV), as determined in a previous work [39], and in the same order of values corresponding to the anatase and rutile crystalline phases of TiO_2 [47]. On the other hand, the incorporation of mass percentages of CQDs-CAU higher than 4% (*w/w*) into TiO_2 resulted in increasing band gap energies of the resulting TiO_2/CQDs-CAU composites (as reported elsewhere [39]), which might explain the better photocatalytic performance of TiO_2/CQDs-CAU 4% (*w/w*) as compared with TiO_2/CQDs-CAU 5% (*w/w*), TiO_2/CQDs-CAU 6% (*w/w*) and TiO_2/CQDs-CAU 8% (*w/w*). It is to highlight that TiO_2/CQDs-CA 4% (*w/w*) was also the most efficient of the composites with CQDs-CA (Fig. 1). These results confirm those previously observed by Silva et al. [39] for the photocatalytic removal of oxolinic acid using TiO_2/CQDs composites with 4% (*w/w*) CQDs content (these being more efficient than the ones with larger percentages (from 5% to 8% (*w/w*)). This is in agreement with other authors that also found that photocatalytic performance of TiO_2/CQDs composites is not associated to larger CQDs contents [34,36,37].

As for the most efficient materials for each antibiotic, the results for SDZ showed that, in PBS (Fig. 1 a)), TiO_2/CQDs-CA 4% (*w/w*) was the most efficient photocatalysts for SDZ, attaining a C/C_0 of 0.33 ± 0.08 after irradiation during 0.3 h. Meanwhile, in SSS (Fig. 1 a)), CQDs-CAUC followed by the composite TiO_2/CQDs-CAU 4% (*w/w*) were the most efficient, with a C/C_0 of 0.53 ± 0.03 and 0.64 ± 0.02, respectively, after 0.3 h under irradiation.

The results presented in Fig. 1 b_1) showed that in PBS, after 4 h of irradiation, four photocatalysts (TiO_2C, TiO_2/CQDs-CA 4% (*w/w*), TiO_2/CQDs-CAU 4% (*w/w*), TiO_2/CQDs-CAU 5% (*w/w*)) allowed for a complete removal of SMX (the SMX concentration in the irradiated solutions were lower than the LOD). In order to choose between these four photocatalysts, the experiment was repeated but irradiating during 0.25 h. Results, presented in Fig. 1 b_2), demonstrated that TiO_2/CQDs-CAU 4% (*w/w*) was the most efficient photocatalysts for SMX photodegradation in PBS with C/C_0 of 0.66 ± 0.08. Meanwhile, in SSS (Fig. 1 b_1)), TiO_2/CQDs-CAU 4% (*w/w*) and TiO_2/CQDs-CAU 6% (*w/w*), with C/C_0 of 0.48 ± 0.02 and 0.48 ± 0.03, respectively, were the most efficient for SMX.

Lastly, for TMP, the results in PBS (Fig. 1 c)) showed that TiO_2/CQDs-CAU 4% (*w/w*) was the only photocatalyst that provided an antibiotic concentration below LOD under irradiation for 2 h. Therefore, TiO_2/CQDs-CAU 4% (*w/w*) was selected as the most efficient photocatalyst for TMP photodegradation. In SSS (Fig. 1 c)), TiO_2/CQDs-CAU 4% (*w/w*) was also the most efficient with C/C_0 of 0.600 ± 0.009 for TMP after 1 h of irradiation.

According to the obtained results, Table 1 presents a summary of the selected photocatalysts for each antibiotic and each matrix to be used in subsequent experiments.

3.2. Photocatalysts' dosage optimization

After selecting the most efficient photocatalysts for each antibiotic and matrix, their dosages were optimized. The photodegradation results of SDZ, SMX and TMP in PBS and SSS, for the tested photocatalyst dosages are presented in Fig. 2. It is necessary to refer that no differences were observed between the initial concentration (stock solution) of SDZ, SMX or TMP and that in the dark controls, indicating that the decrease of antibiotic observed in the irradiated solutions was only due to photodegradation processes. However, depending on the antibiotic, its concentration, matrix and photocatalyst, differences on the degradation results obtained at different dosages were observed. These results underline the importance of optimizing the photocatalyst concentration necessary for the treatment of aquaculture effluents considering the specific conditions, which is imperative to minimize resources' consumption, from practical, economic and environmental points of view.

For 10 mg L^{-1} SDZ in PBS (Fig. 2 a_1), results evidenced an increase of photodegradation with the increase of TiO_2/CQDs-CA 4% (*w/w*) dosage. For 0.3 h of irradiation, the highest degradation was obtained using 500 mg L^{-1} TiO_2/CQDs-CA 4% (*w/w*) (C/C_0 of 0.22 ± 0.01) and 1000 mg L^{-1} of TiO_2/CQDs-CA 4% (*w/w*) (C/C_0 was 0.09 ± 0.01). Since the photodegradation was particularly high in such a small irradiation period (0.3 h), the possible gain in the irradiation time needed for total degradation when doubling the photocatalyst dose from 500 to 1000 mg L^{-1} was not considered advantageous. For this reason, 500 mg L^{-1} TiO_2/CQDs-CA 4% (*w/w*) was the condition selected.

Results obtained for SDZ photocatalysis in SSS (Fig. 2 a_2)) using CQDs-CAUC and TiO_2/CQDs-CAU 4% (*w/w*), also demonstrated an increase in the photodegradation with the photocatalyst dosage. In the case of CQDs-CAUC, no significant differences were observed between C/C_0 obtained using 1000 mg L^{-1} (0.26 ± 0.02) or 500 mg L^{-1} (0.31 ± 0.03) of CQDs-CAUC. However, this was not the case for the composite, with 1000 mg L^{-1} of TiO_2/CQDs-CAU 4% (*w/w*) providing

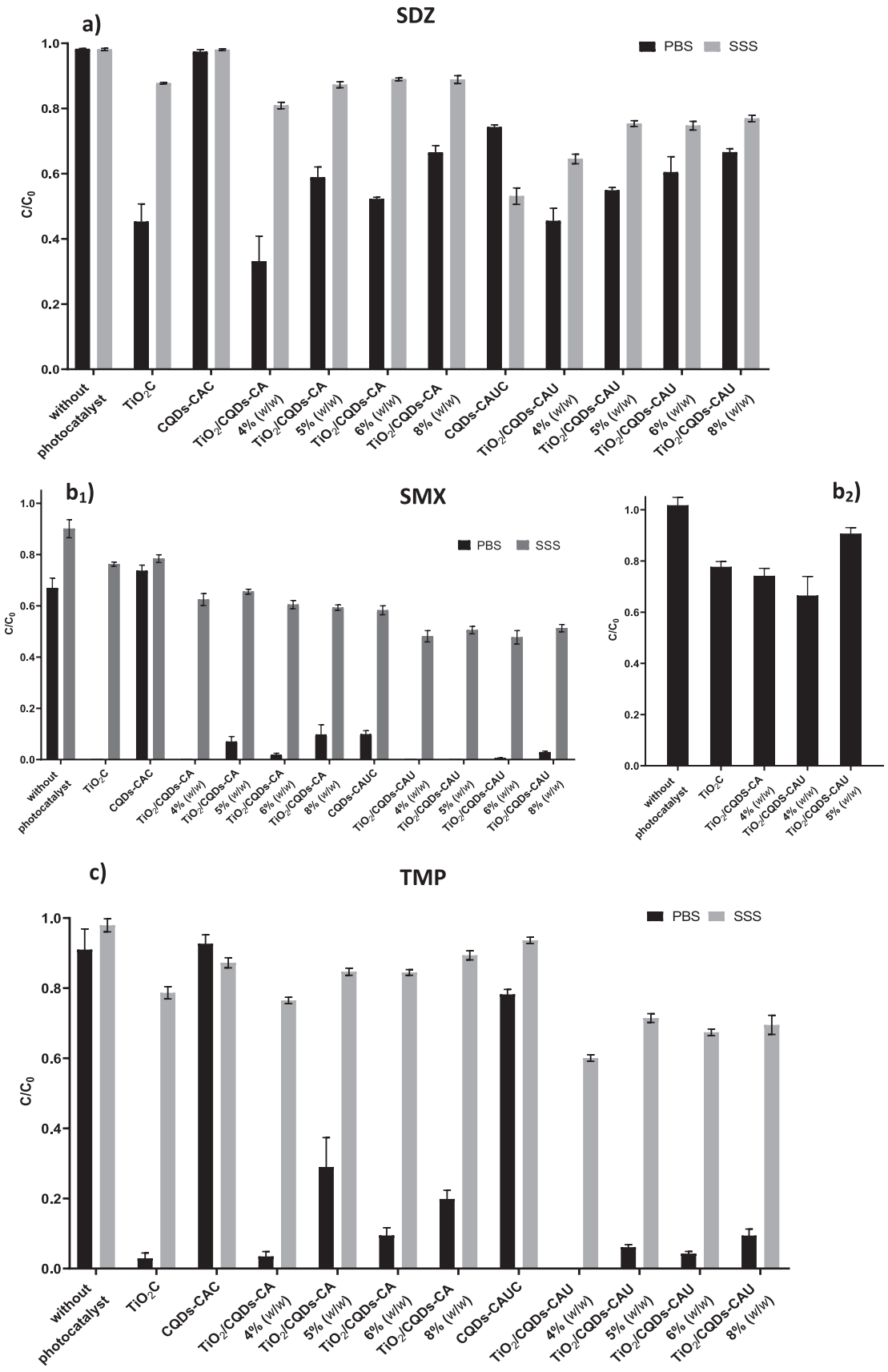

Fig. 1. Photolysis and photocatalytic degradation of (a) SDZ in PBS and SSS, with 250 mg L^{-1} of photocatalyst for 0.3 h of irradiation; (b) SMX with 100 mg L^{-1} of photocatalyst in (b_1) PBS (4 h of irradiation) and SSS (2 h of irradiation), and (b_2) PBS (0.25 h of irradiation); (c) TMP with 100 mg L^{-1} of photocatalyst in PBS (2 h of irradiation) and SSS (1 h of irradiation). Each bar represents triplicate experiments (mean ± standard deviation (n = 3)).

Table 1
Summary of the photocatalysts chosen for each antibiotic and each matrix.

Antibiotic	*Matrix*	*Photocatalysts*
SDZ	PBS	TiO_2/CQDs-CA 4% (*w/w*)
	SSS	CQDs-CAUC and TiO_2/CQDs-CAU 4% (*w/w*)
SMX	PBS	TiO_2/CQDs-CAU 4% (*w/w*)
	SSS	TiO_2/CQDs-CAU 4% (*w/w*) and TiO_2/CQDs-CAU 6% (*w/w*)
TMP	PBS	TiO_2/CQDs-CAU 4% (*w/w*)
	SSS	TiO_2/CQDs-CAU 4% (*w/w*)

significantly lower C/C_0 (0.349 ± 0.006) and therefore being the selected dosage for subsequent kinetic studies. Regarding SMX in PBS (Fig. 2 b_1)), the increase in TiO_2/CQDs-CAU 4% (*w/w*) dosage also resulted in an increase of the photodegradation rate, with a minimum of C/C_0 of 0.17 ± 0.02 for SMX photodegradation in 0.25 h when using 500 mg L^{-1} photocatalyst. However, the small increase observed between the use of 200 and 500 mg L^{-1} does not justify the extra amount of photocatalyst applied. For this reason, 200 mg L^{-1} TiO_2/CQDs-CAU 4% (*w/w*) was considered more adequate and thus selected for the subsequent experiments on the photocatalysis of SMX in PBS.

Using the two selected photocatalysts (TiO_2/CQDs-CAU 4% (*w/w*) and TiO_2/CQDs-CAU 6% (*w/w*)) for SMX degradation in SSS (Fig. 2 b_2)) provided, after 0.5 h of irradiation, a decrease of C/C_0 with the increase of the photocatalyst dosage for both materials, especially up to

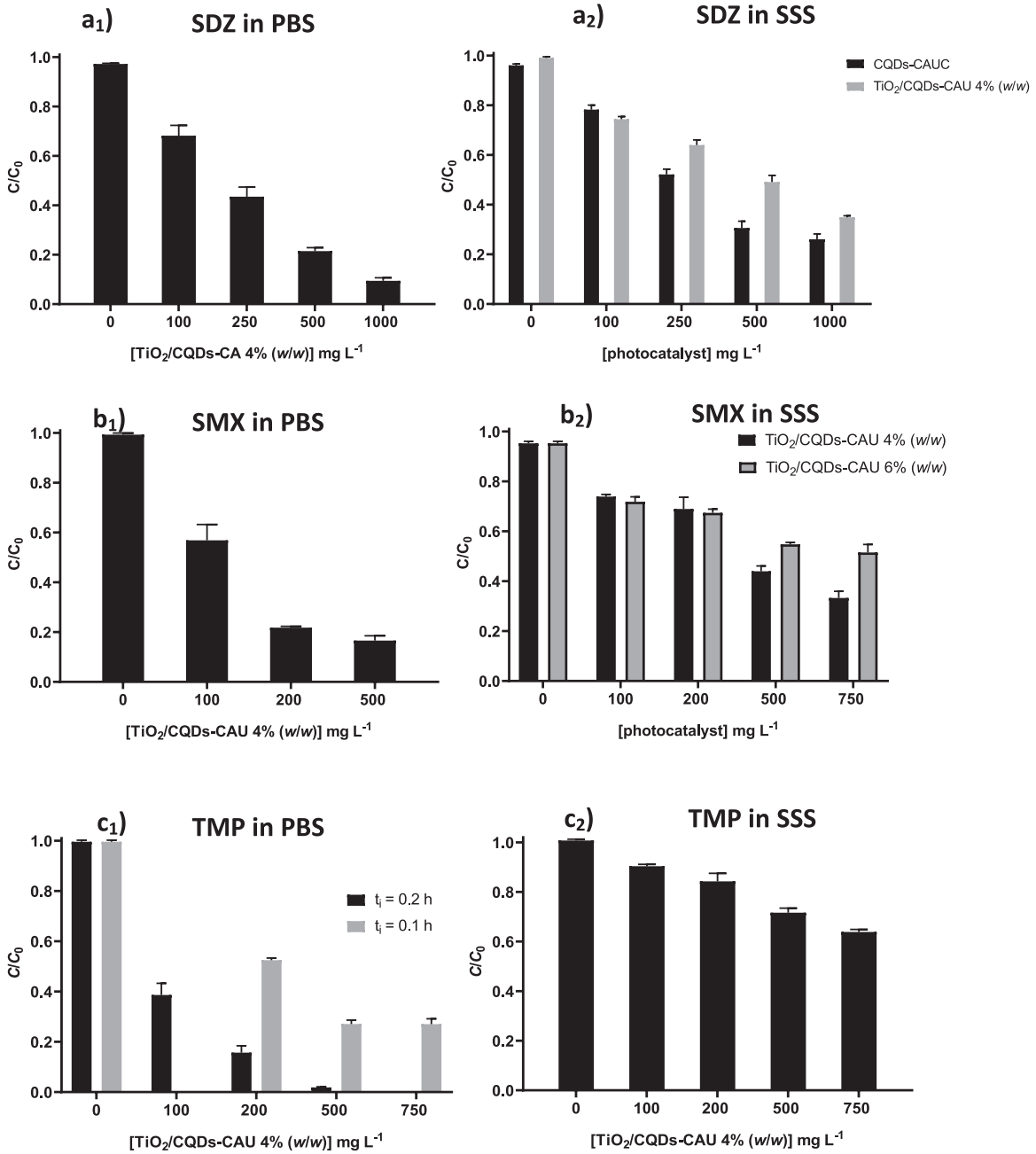

Fig. 2. Photocatalyst dosage study for 10 mg L^{-1} of (a) SDZ after 0.3 h of irradiation in (a_1) PBS and (a_2) SSS; (b) SMX in (b_1) PBS after 0.25 h of irradiation and (b_2) SSS after 0.5 h of irradiation; (c) TMP after 0.25 h of irradiation in (c_1) PBS and (c_2) SSS. Each bar represents triplicate experiments (mean ± standard deviation (n = 3)).

500 mg L^{-1}. Comparing the two photocatalysts at 500 mg L^{-1}, TiO_2/CQDs-CAU 4% (*w/w*) was selected as the most efficient photocatalyst ($C/C_0 = 0.44 \pm 0.02$) and this the dosage to be applied in the kinetic studies.

Results obtained for TMP in PBS (Fig. 2 c_1)) after 0.2 h of irradiation demonstrated an increase in the photodegradation rate with the increase of TiO_2/CQDs-CAU 4% (*w/w*) up to 500 mg L^{-1}. In order to increase even more the concentration of photocatalyst, irradiation time was reduced to 0.1 h and concentrations tested before (200 and 500 mg L^{-1}) were evaluated again and compared with the results determined using 750 mg L^{-1}. Results obtained at 500 and 750 mg L^{-1} were not significantly different, so 500 mg L^{-1} TiO_2/CQDs-CAU 4% (*w/w*) was the chosen dosage.

For TMP in SSS an increase of photodegradation with the increase of TiO_2/CQDs-CAU 4% (*w/w*) dosage (Fig. 2 c_2)) was observed, with a maximum photodegradation for 750 mg L^{-1}, with C/C_0 of 0.64 ± 0.01 in 0.25 h. However, using 500 mg L^{-1}, a C/C_0 of 0.72 ± 0.02 was obtained. As before, the extra amount of photocatalyst necessary for the small degradation increase observed at 750 mg L^{-1} in comparison with 500 mg L^{-1} was not considered worthwhile, so 500 mg L^{-1} TiO_2/CQDs-

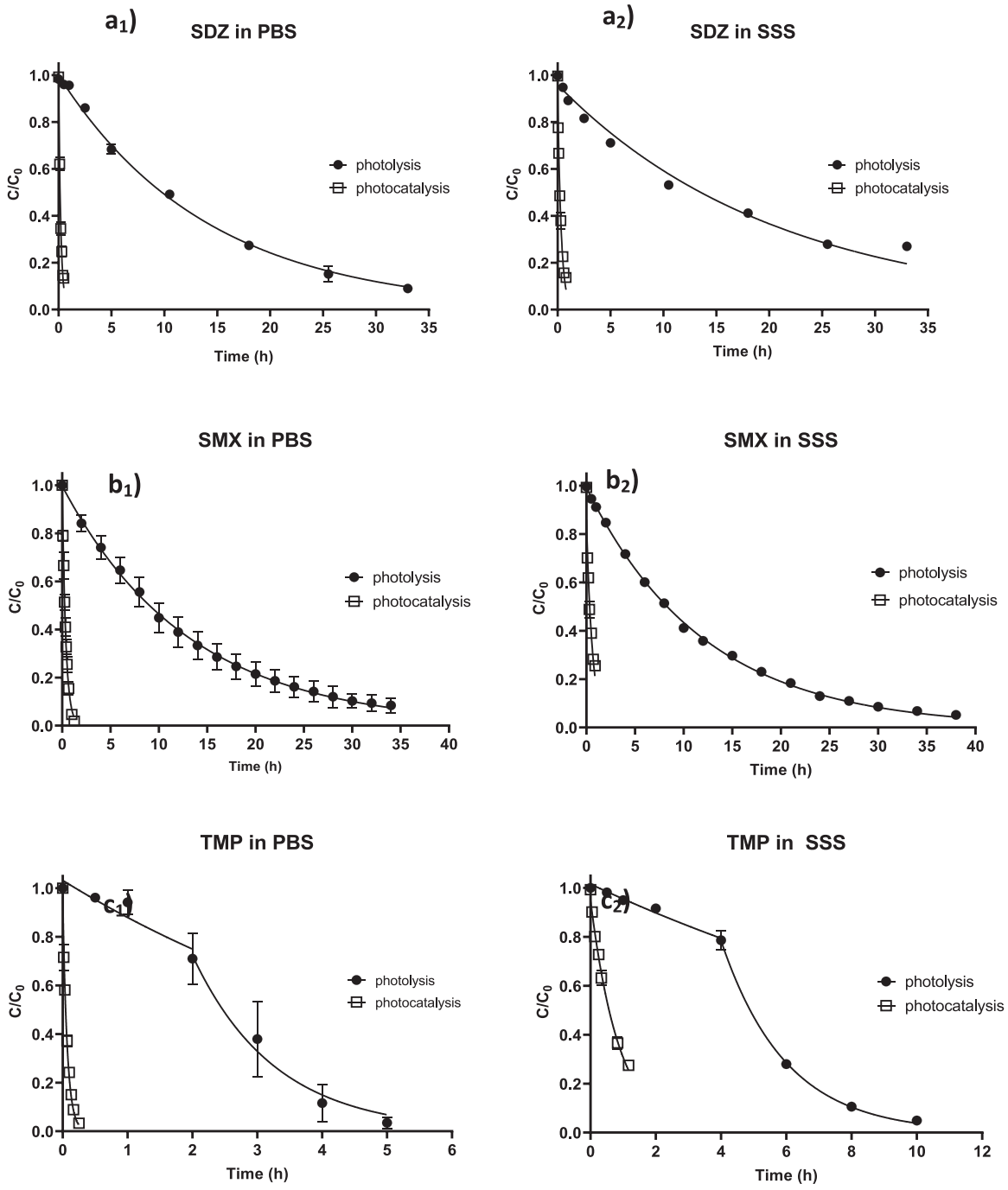

Fig. 3. Kinetic experimental data together with fittings to the pseudo first-order equation for the photodegradation of (a_1) 10 mg L^{-1} SDZ in PBS in absence and presence of 500 mg L^{-1} TiO_2/CQDs-CA 4% (w/w) and (a_2) 10 mg L^{-1} SDZ in SSS in absence and presence of 1000 mg L^{-1} TiO_2/CQDs-CA 4% (w/w); (b_1) 10 mg L^{-1} SMX in PBS in absence and presence of 200 mg L^{-1} TiO_2/CQDs-CAU 4% (w/w) and (b_2) 10 mg L^{-1} SMX in SSS in absence and presence of 500 mg L^{-1} TiO_2/CQDs-CAU 4% (w/w); (c_1) 10 mg L^{-1} TMP in PBS in absence and presence of 500 mg L^{-1} TiO_2/CQDs-CAU 4% (w/w) and (c_2) 10 mg L^{-1} TMP in SSS in absence and presence of 500 mg L^{-1} TiO_2/CQDs-CAU 4% (w/w). Note: The scales of the xx axes are different for a better visualization of the results.

CAU 4% (*w/w*) was the selected dosage for TMP photocatalysis experiments in SSS.

3.3. Photodegradation kinetics

For each antibiotic, photodegradation kinetic studies were carried out in each matrix, either in absence and presence of the selected photocatalyst and respective dosage. The photodegradation kinetic curves of SDZ, SMX and TMP in each matrix are presented in Fig. 3. Experimental results obtained in PBS and SSS for SDZ and SMX photolysis and photocatalysis using the selected TiO_2/CQDs composites were satisfactorily described by the pseudo first-order kinetic equation, as shown in Fig. 3 a) and b), respectively. The corresponding kinetic parameters from the fittings of experimental data to the pseudo first-order equation, namely k (h^{-1}) and R^2, are given in Table 2 together with the determined $t_{1/2}$ (h).

The matrix may influence the photodegradation rate of each antibiotic, either in presence or absence of photocatalyst. In SSS, where ionic concentration is relatively higher, ions may stimulate antibiotics photodegradation by producing reactive oxygen species (*e.g.*, •OH, $•CO^{3-}$, •HCO or $•O^-$) [48] or inhibit photodegradation by different processes, mainly scavenging •OH by halogen ions (Cl^- and Br^-) [49,50] and complexation with ions such as Ca^{2+} or Mg^{2+} [18].

SDZ photodegradation kinetic curves in PBS and SSS without photocatalyst (Fig. 3 a_1) and a_2)) were quite similar. Notwithstanding, the fitted k and the calculated $t_{1/2}$ in Table 2 point to a slightly faster degradation in PBS, which may be related to the slight dominance of salinity inhibitory effects. Furthermore, Fig. 3 a_1) and a_2) evidence that, in both matrices, SDZ photodegradation occurred much faster in the presence of the selected photocatalyst. Regarding the k in PBS, it increased from 7.09×10^{-2} h^{-1} in absence of photocatalyst to 4.81 h^{-1} in presence of TiO_2-CQDs-CA 4% (*w/w*). Meanwhile, in SSS the k increased from 4.84×10^{-2} h^{-1} to 3.04 h^{-1} in presence of TiO_2-CQDs-CAU 4% (*w/w*). In agreement with the k values, the highest $t_{1/2}$ for SDZ (Table 2) was obtained without photocatalyst in SSS (14.3 h). In presence of the selected photocatalyst, the lowest $t_{1/2}$ was obtained in PBS (0.144 h).

Table 3 presents a comparison of literature data for the photodegradation of each antibiotic and the herein presented results. As it may be seen, comparing with the most recent results on SDZ photocatalytic degradation, the here synthesized TiO_2/CQDs-CA 4% (*w/w*) and TiO_2/CQDs-CAU 4% (*w/w*) were among the most efficient photocatalysts. In fact, Chen et al. [22] used 100 mg L^{-1} of AQ_2S@rGO system for the photodegradation of 10 mg L^{-1} SDZ (pH 7, 0.5 mol L^{-1} NaCl) obtaining a k of 1.789 h^{-1}. Meanwhile, Evgenidou et al. [51] tested Cu-modified TiO_2 photocatalysts (100 mg L^{-1}) for the photodegradation of a mixture of eight antibiotics and obtained a k of 11.0 ± 0.6 h^{-1} for a solution of 1 mg L^{-1} SDZ in ultrapure water. Finally, Silva et al. [24] observed that 100 mg L^{-1} biochar-TiO_2 magnetic nanocomposites increased SDZ (10 mg L^{-1}) photodegradation k from 0.062 h^{-1} to 0.236 h^{-1}. Although the same experimental conditions would be desirable for an accurate comparison of results, it is possible to state that the photocatalysts synthesized in this study were remarkably efficient in the removal of SDZ.

Regarding SMX, photodegradation kinetics without photocatalyst was very similar in PBS and in SSS (Fig. 3 b_1) and b_2)), with the respective $t_{1/2}$ being 9.06 and 8.38 h (Table 2). Differently from SDZ, salinity net effect on SMX was the promotion of photodegradation. However, as for SDZ, SMX photodegraded much faster in presence of the selected photocatalyst, namely TiO_2/CQDs-CAU 4% (*w/w*) (Fig. 3 b_1) and b_2)). This is evident by the increase of k in PBS from 7.65×10^{-2} to 2.72 h^{-1} and in SSS from 8.27×10^{-2} to 1.60 h^{-1} (Table 2). The utilization of TiO_2/CQDs-CAU 4% (*w/w*) as photocatalyst allowed to obtain very short $t_{1/2}$ for SMX either in PBS (0.255 h) or in SSS (0.43 h), which were significantly lower than in absence of photocatalyst, especially in PBS (9.06 h). A recent compilation on SMX degradation using TiO_2-based photocatalysts by Kutuzova et al. [52] reported k values between 0.26 and 63 h^{-1}. Although the experimental conditions were different, it may be observed that TiO_2/CQDs-CAU 4% (*w/w*) provided values within this range. Also, as shown in Table 3, Malesic-Eleftheriadou et al. [53] used biobased-PET-TiO_2 P25 composite films (500 mg L^{-1}) for the photodegradation of a 1 mg L^{-1} SMX solution in ultrapure water and obtained a k of 0.9 h^{-1} and a $t_{1/2}$ of 0.77 h. On the other hand, Porcar-Santos et al. [54] used 100 mg L^{-1} of TiO_2 P25 (Degussa) for the photodegradation of 1 mg L^{-1} SMX in deionized water (pH 6.0) and simulated seawater (pH 8.2), the k values being 2.46 h^{-1} and 1.2 h^{-1}, respectively, which are much lower than the values here obtained with TiO_2/CQDs-CAU 4% (*w/w*) in PBS and SSS.

Finally, comparing results in Fig. 3 c_1) and c_2), it is evident that in absence of photocatalyst, TMP photodegradation occurred much faster in PBS than in SSS, where inhibitory effects related to the scavenging of •OH by Cl^- and Br^- and complexation must have been dominant. It is important to highlight that TMP photolysis in both matrices was not properly described by the pseudo first-order kinetic equation. This was already observed by Sirtori et al. [55], who reported that this behaviour could be due to the occurrence of several degradation mechanisms, including an initial slow reaction by direct irradiation and a second faster mechanism promoted by the creation of a photoreactive intermediate (trimethoxybenzoylpyrimidine), producing an autocatalytic effect. On the other hand, Mathon et al. [56] fitted the results of TMP photolysis in ultrapure water to pseudo first-order kinetic equation; however, kinetics results were not shown. In this study, and in order to compare results, TMP photolysis kinetic experimental curves were divided into two consecutive stages and each one was fitted to the pseudo first-order kinetic equation, the corresponding k values being presented in Table 2**.** The slower photodegradation of TMP in presence of salts was also observed by Sirtori et al. [55], who studied the direct photolysis of this antibiotic in demineralised and simulated seawater.

Under the presence of 500 mg L^{-1} TiO_2/CQDs-CAU 4% (*w/w*), TMP photodegradation significantly accelerated in both matrices and results fitted the pseudo-first order kinetic equation. Kutuzova et al. [52] recently revised the literature on the TiO_2-based photocatalysts applied to TMP and reported k values between 0.06 and 39.6 h^{-1}. Meanwhile, in this work, TiO_2/CQDs-CAU 4% provided k values of 14.6 and 1.13 h^{-1}

Table 2
Data on pseudo-first order rate constants (k (h^{-1})), determination coefficient (R^2) and half-life times ($t_{1/2}$ (h)) obtained for the photodegradation of 10 mg L^{-1} of antibiotic in PBS and SSS in absence and presence of the most efficient photocatalyst. Note: SD is the standard deviation (n = 3).

Sample	k ± SD (h^{-1})		R^2	$t_{1/2}$ ± SD (h)
SDZ in PBS	(7.09 ± 0.09)× 10^{-2}		0.999	9.78 ± 0.12
SDZ in PBS + 500 mg L^{-1} TiO_2/CQDs-CA 4%	4.81 ± 0.06		0.993	0.144 ± 0.002
SDZ in SSS	(4.84 ± 0.10)× 10^{-2}		0.981	14.3 ± 0.3
SDZ in SSS + 1000 mg L^{-1} TiO_2/CQDs-CAU 4%	3.04 ± 0.07		0.984	0.228 ± 0.005
SMX in PBS	(7.65 ± 0.08)× 10^{-2}		0.999	9.06 ± 0.09
SMX in PBS + 200 mg L^{-1} TiO_2/CQDs-CAU 4%	2.72 ± 0.06		0.999	0.255 ± 0.006
SMX in SSS	(8.27 ± 0.03)× 10^{-2}		0.999	8.38 ± 0.03
SMX in SSS + 500 mg L^{-1} TiO_2/CQDs-CAU 4%	1.60 ± 0.06		0.949	0.43 ± 0.02
TMP in PBS	0–2 h	0.16 ± 0.05	0.873	Not determined
	2–5 h	0.8 ± 0.1	0.982	Not determined
TMP in PBS + 500 mg L^{-1} TiO_2/CQDs-CAU 4%	14.6 ± 0.6		0.996	0.047 ± 0.002
TMP in SSS	0–4 h	0.062 ± 0.003	0.917	Not determined
	4–10 h	0.50 ± 0.01	0.995	Not determined
TMP in SSS + 500 mg L^{-1} TiO_2/CQDs-CAU 4%	1.13 ± 0.06		0.990	0.61 ± 0.01

Table 3
Literature studies on the photocatalytic degradation of SDZ, SMX and TMP.

Antibiotic	[Antibiotic] (mg L^{-1})	Matrix	Light source	Photocatalyst	[Photocatalyst] (mg L^{-1})	k (h^{-1})	Ref.
SDZ	10	PBS	simulated solar light irradiation 55 W m^{-2} (290–400 nm)	*TiO_2/CQDs-CA 4% (w/w)*	500	4.81 ± 0.06	This study
		SSS		*TiO_2/CQDs-CAU 4% (w/w)*	1000	3.04 ± 0.07	
	10	0.5 mol L^{-1} NaCl, pH 7	simulated solar light irradiation 60 mW cm^{-2} (320–780 nm)	AQ_2S@rGO	100	1.782	[22]
	1	Ultrapure water	simulated solar light irradiation 500 W m^{-2} (300–800 nm)	Cu-modified TiO_2	100	11.0 ± 0.6	[51]
	10	0.001 mol L^{-1} phosphate buffer, pH 7.3	simulated solar light irradiation 55 W m^{-2} (290–400 nm)	biochar-TiO_2 magnetic	100	0.062–0.236	[24]
SMX	10	PBS	simulated solar light irradiation 55 W m^{-2} (290–400 nm)	*TiO_2/CQDs-CAU 4% (w/w)*	200	2.72 ± 0.06	This study
		SSS		*TiO_2/CQDs-CAU 4% (w/w)*	500	1.60 ± 0.06	
	1	ultrapure water	solar simulator, Xenon lamp (1.5 kW) 500 W m^{-2}	biobased-PET-TiO_2 P25 composite films	500	0.9	[53]
	1	deionized water, pH 6.0	solar simulation chamber, Xenon lamp (1.5 kW) (290–400 nm)	TiO_2 P25 (Degussa)	100	2.46	[54]
		simulated seawater, pH 8.2				1.2	
TMP	10	PBS	simulated solar light irradiation 55 W m^{-2} (290–400 nm)	*TiO_2/CQDs-CAU 4% (w/w)*	500	14.6 ± 0.6	This study
		SSS		*TiO_2/CQDs-CAU 4% (w/w)*	500	1.13 ± 0.06	
	15×10^{-6}	treated wastewater	simulated solar light irradiation 500 W m^{-2} (350–840 nm)	TiO_2 powder	500	(100% removal after 3 h)	[57]
	121×10^{-3}	hospital wastewater	UV irradiation	porous geopolymer composite membranes with TiO_2 (10 *wt* %)	25000	0.108	[58]

for TMP in PBS and SSS, respectively. As depicted in Table 3, both Felis et al. [57] and Sanguanpak et al. [58] recently studied the photocatalysis of TMP in real water matrices, treated municipal wastewater sample and hospital wastewater. Felis et al. [57] applied 500 mg L^{-1} of TiO_2 powder for the photocatalysis of around 15 ng L^{-1} of TMP, attaining a complete removal (100%) after 3 h. On the other hand, Sanguanpak et al. [58] produced porous geopolymer composite membranes with optimal TiO_2 immobilization (10 *wt*%) and applied 25 g L^{-1} for the removal of 121 μg L^{-1} TMP (determined concentration in hospital wastewater), with a smaller photodegradation rate (k of 0.108 h^{-1}) than the herein obtained.

3.4. Final remarks

Two different procedures, both using non-toxic, inexpensive and easily available precursors, were followed in this work for the production of CQDs. Comparing both procedures, the synthesis of CQDs-CA included a longer thermal treatment than that of CQDs-CAU (40 h vs. 5 h at 180 °C), but the production yield of CQDs-CA (51%) was higher than that of CQDs-CAU (37%). As for the incorporation of either CQDs-CA or CQDs-CAU on TiO_2, hydrothermal calcination (300 °C during 3 h) was carried out, which is the most demanding stage of the composites' production in terms of energy. Although the production of CQDs is considered to be facile, rapid and aligned with the principles of green chemistry, there is limited information about the impacts of their synthesis and still less on the synthesis of TiO_2/CQDs composites. For such information, life cycle assessment (LCA) is an approach that has been used with success to evaluate the environmental impacts associated with different engineered nanomaterials, including CQDs [59]. In view of scaling-up, a cradle-to-cradle assessment, including all stages (from the provision of raw materials to product use and disposal), would be worthwhile to select the most favourable procedures and materials in terms of efficiency and sustainability.

As for the performance, obtained results evidenced that, under simulated sunlight, photocatalysis using the here synthesized TiO_2/CQDs allowed for much more efficient removals of SDZ, SMX and TMP than photolysis, either in simulated fresh or brackish water. In general, CQDs-CAU provided larger efficiency than CQDs-CA, which must be related to N-doping. Among the produced composites, TiO_2/CQDs-CAU 4% (*w/w*) was the most efficient photocatalyst for SMX and TMP, in either PBS or SSS, and for SDZ in SSS. Meanwhile, for SDZ in PBS, TiO_2/CQDs-CA 4% (*w/w*), followed by TiO_2/CQDs-CAU 4% (*w/w*), displayed the best performance. Therefore, the introduction of CQDs in TiO_2 at 4% (*w/w*) provided more efficient photocatalysts than the introduction of higher CQDs % (*w/w*) (from 5% to 8% (*w/w*)), so confirming previous observations for the photocatalytic removal of oxolinic acid [39]. Moreover, results point to TiO_2/CQDs-CAU 4% (*w/w*) as the composite of choice for a photocatalytic treatment of aquaculture effluents aimed at the removal of antibiotics. Although the selected photocatalysts allowed for remarkably higher k and lower $t_{1/2}$ than photolysis in either PBS or SSS, it was observed that the water matrix largely affected the photocatalysts performance, pointing to the importance of evaluations such as the one carried out in this work for any specific application.

Overall, in literature, the evaluation of photocatalysts for antibiotics removal from water is applied to a limited number of antibiotics (usually one and no more than two) and/or conditions (usually one and no more than two matrices, normally not including a saline matrix). In this study, three antibiotics and two different matrices (representing fresh and brackish water) were studied. The efficient removal from both matrices is a great indication for the promising application of the produced TiO_2/CQDs composites in real effluents from aquaculture. In this sense, it should be highlighted that the produced materials present many advantages: they are low cost, simple to produce, easy to use and allow for their recovery by decantation which, in turn, allow for their reutilization. Moreover, the excellent efficiency under solar radiation lowers the price of the up-scaled implementation since it does not require UV light/radiation. Additionally, since both SMX and TMP have been detected in urban and hospital wastewater, a further application of the herein tested materials could be the tertiary treatment stage of municipal wastewater treatment plants, showing the diversified application of the synthesized

photocatalysts.

However, considering the main contribution of this work - pointing to CQDs/TiO_2 composites as promising photocatalysts for the photocatalytic removal of antibiotics from aquaculture effluents under sunlight - several questions are still unsolved. Further research needs to be carried out on these antibiotics' photodegradation pathways and photoproducts in the different matrices in order to determine the photodegradation mechanisms and uncover the reasons beneath the divergences observed in the efficiencies for the different antibiotics and matrices. In addition, the assessment of the mineralization achieved by the composites, the evaluation of antibacterial activity and/or photoproducts toxicity should be analysed for a complete assessment on their performance. Finally, and taking into account that selectivity may be a relevant issue in complex matrices such as aquaculture effluents, photocatalytic experiments in real samples need to be done in order to prove the efficiency of CQDs/TiO_2 composites.

4. Conclusion

Most of the synthesized TiO_2/CQDs composites, especially those with a 4% (*w*/*w*) content of CQDs, demonstrated that their presence in solution accelerated the photodegradation of SDZ, SMX and TMP, comparatively to photolysis. Among them, TiO_2/CQDs-CAU 4% (*w*/*w*) was the most efficient for the removal of SMX and TMP, either in PBS or SSS, and SDZ in SSS. Meanwhile, for the removal of SDZ in PBS, TiO_2/CQDs-CA 4% (*w*/*w*), followed by TiO_2/CQDs-CAU 4% (*w*/*w*), was the most efficient. Furthermore, differences in the photocatalysts' efficiency in PBS and SSS indicated that the matrix influences the photodegradation efficiency of the TiO_2/CQDs composites. As compared with photolysis, kinetic studies showed that the use of the selected composites and dosages allowed for a drastic decrease of the $t_{1/2}$ from 9.78 h to 0.144 h for SDZ in PBS, from 14.3 h to 0.228 h for SDZ in SSS, from 9.06 h to 0.255 h for SMX in PBS and from 8.38 h to 0.43 h for SMX in SSS. Although TMP photolysis did not fit pseudo-first order kinetics, the decrease in the time needed to photodegrade this antibiotic using 500 mg L^{-1} TiO_2/CQDs-CAU 4% (*w*/*w*) was evident, with a $t_{1/2}$ of 0.047 h and 0.61 h in PBS and SSS, respectively. Therefore, the results herein reported indicate that the utilization of solar driven photocatalysis using TiO_2/CQDs composites, with TiO_2/CQDs-CAU 4% (*w*/*w*) displaying the most remarkable performance, may be a suitable solution to remove SDZ, SMX and TMP from aquaculture (fresh and brackish) effluents.

CRediT authorship contribution statement

Valentina Silva: Investigation, Formal Analysis, Methodology, Writing - Original Draft. **Joana F.A. Fernandes**: Investigation, Writing - Review & Editing. **Maria Clara Tomás**: Investigation, Writing - Review & Editing. **Carla Patrícia Silva**: Conceptualization, Methodology, Writing - Review & Editing, Supervision. **Vânia Calisto**: Conceptualization, Methodology, Writing - Review & Editing, Supervision, Resources, Funding acquisition. **Marta Otero**: Conceptualization, Methodology, Formal analysis, Writing - Review & Editing, Supervision, Resources, Funding acquisition. **Diana L.D. Lima**: Conceptualization, Methodology, Formal analysis, Writing - Original Draft, Writing - Review & Editing, Supervision, Resources, Funding acquisition.

Declaration of Competing Interest

The authors declare that they have no known competing financial interests or personal relationships that could have appeared to influence the work reported in this paper.

Data Availability

Data will be made available on request.

Acknowledgments

This work was funded by FEDER through CENTRO 2020 and by national funds through Fundação para a Ciência e a Tecnologia (FCT) within the research project PTDC/ASP-PES/29021/2017. Valentina Silva thank support by FCT PhD grant (2022.10472.BD). Diana Lima acknowledges funding from FCT under the Scientific Employment Stimulus (2022.00570.CEECIND). We acknowledge financial support to CESAM by FCT/MCTES (UIDP/50017/2020 +UIDB/50017/2020 + LA/P/0094/2020), through national funds.

Appendix A. Supporting information

Supplementary data associated with this article can be found in the online version at doi:10.1016/j.cattod.2023.114150.

References

[1] E. Emmanuel, Y. Perrodin, G. Keck, J.-M. Blanchard, P. Vermande, Ecotoxicological risk assessment of hospital wastewater: a proposed framework for raw effluents discharging into urban sewer network, J. Hazard. Mater. 117 (2005) 1–11, https://doi.org/10.1016/j.jhazmat.2004.08.032.

[2] M. Seoane, C. Rioboo, C. Herrero, A. Cid, Toxicity induced by three antibiotics commonly used in aquaculture on the marine microalga Tetraselmis suecica (Kylin) Butch, Mar. Environ. Res. 101 (2014) 1–7, https://doi.org/10.1016/j.marenvres.2014.07.011.

[3] L. Granada, N. Sousa, S. Lopes, M.F.L. Lemos, Is integrated multitrophic aquaculture the solution to the sectors' major challenges? - a review, Rev. Aquacult 8 (2016) 283–300, https://doi.org/10.1111/raq.12093.

[4] K. Grigorakis, G. Rigos, Aquaculture effects on environmental and public welfare – the case of Mediterranean mariculture, Chemosphere 85 (2011) 899–919, https://doi.org/10.1016/j.chemosphere.2011.07.015.

[5] R. Lulijwa, E.J. Rupia, A.C. Alfaro, Antibiotic use in aquaculture, policies and regulation, health and environmental risks: a review of the top 15 major producers, Rev. Aquac. 12 (2020) 640–663, https://doi.org/10.1111/raq.12344.

[6] H.-T. Lai, J.-J. Lin, Degradation of oxolinic acid and flumequine in aquaculture pond waters and sediments, Chemosphere 75 (2009) 462–468, https://doi.org/10.1016/j.chemosphere.2008.12.060.

[7] R. Zhang, Y. Kang, R. Zhang, M. Han, W. Zeng, Y. Wang, K. Yu, Y. Yang, Occurrence, source, and the fate of antibiotics in mariculture ponds near the Maowei Sea, South China: storm caused the increase of antibiotics usage, Sci. Total Environ. 752 (2021), 141882, https://doi.org/10.1016/j.scitotenv.2020.141882.

[8] World Health Organization, World Health Organization model list of essential medicines: 22nd list (2021), World Health Organization, 2021. https://apps.who.int/iris/handle/10665/345533 (Accessed 19 December 2022).

[9] Z. Wang, Y. Li, X. Liang, S. Zhang, W. Shi, J. Shen, Forcing immunoassay for sulfonamides to higher sensitivity and broader detection spectrum by site heterologous hapten inducing affinity improvement, Anal. Methods 5 (2013) 6990–7000, https://doi.org/10.1039/C3AY40864G.

[10] Y. Bao, T.-T. Lim, R. Wang, R.D. Webster, X. Hu, Urea-assisted one-step synthesis of cobalt ferrite impregnated ceramic membrane for sulfamethoxazole degradation via peroxymonosulfate activation, Chem. Eng. J. 343 (2018) 737–747, https://doi.org/10.1016/j.cej.2018.03.010.

[11] WHO, World Health Organization [WWW Document] https://www.who.int/, (2020). https://www.who.int (Accessed 9 December 2020).

[12] U.N. UNEP, Frontiers 2017: Emerging Issues of Environmental Concern, UNEP - UN Environment Programme. (2017). http://www.unep.org/resources/frontiers-2017-emerging-issues-environmental-concern (Accessed 21 August 2021).

[13] Y. Ji, C. Ferronato, A. Salvador, X. Yang, J.-M. Chovelon, Degradation of ciprofloxacin and sulfamethoxazole by ferrous-activated persulfate: Implications for remediation of groundwater contaminated by antibiotics, Sci. Total Environ. 472 (2014) 800–808, https://doi.org/10.1016/j.scitotenv.2013.11.008.

[14] P. Chen, Q. Zhang, Y. Su, L. Shen, F. Wang, H. Liu, Y. Liu, Z. Cai, W. Lv, G. Liu, Accelerated photocatalytic degradation of diclofenac by a novel CQDs/BiOCOOH hybrid material under visible-light irradiation: Dechloridation, detoxicity, and a new superoxide radical model study, Chem. Eng. J. 332 (2018) 737–748, https://doi.org/10.1016/j.cej.2017.09.118.

[15] M. Długosz, P. Zmudzki, A. Kwiecień, K. Szczubiałka, J. Krzek, M. Nowakowska, Photocatalytic degradation of sulfamethoxazole in aqueous solution using a floating TiO2-expanded perlite photocatalyst, J. Hazard. Mater. 298 (2015) 146–153, https://doi.org/10.1016/j.jhazmat.2015.05.016.

[16] Q. Sui, J. Huang, S. Deng, W. Chen, G. Yu, Seasonal variation in the occurrence and removal of pharmaceuticals and personal care products in different biological wastewater treatment processes, Environ. Sci. Technol. 45 (2011) 3341–3348, https://doi.org/10.1021/es200248d.

[17] V. Loureiro dos Louros, C.P. Silva, H. Nadais, M. Otero, V.I. Esteves, D.L.D. Lima, Photodegradation of sulfadiazine in different aquatic environments – evaluation of influencing factors, Environ. Res. 188 (2020), https://doi.org/10.1016/j.envres.2020.109730.

[18] C. Oliveira, D.L.D. Lima, C.P. Silva, V. Calisto, M. Otero, V.I. Esteves, Photodegradation of sulfamethoxazole in environmental samples: The role of pH,

organic matter and salinity, Sci. Total Environ. 648 (2019) 1403–1410, https://doi.org/10.1016/j.scitotenv.2018.08.235.
[19] C.P. Silva, C. Oliveira, A. Ribeiro, N. Osório, M. Otero, V.I. Esteves, D.L.D. Lima, Sulfamethoxazole exposure to simulated solar radiation under continuous flow mode: Degradation and antibacterial activity, Chemosphere 238 (2020), 124613, https://doi.org/10.1016/j.chemosphere.2019.124613.
[20] A.A. Gonçalves, G.A. Gagnon, Ozone application in recirculating aquaculture system: an overview, Ozone.: Sci. Eng. 33 (2011) 345–367, https://doi.org/10.1080/01919512.2011.604595.
[21] M. Samy, M.G. Ibrahim, M. Gar Alalm, M. Fujii, Effective photocatalytic degradation of sulfamethazine by CNTs/LaVO4 in suspension and dip coating modes, Sep. Purif. Technol. 235 (2020), 116138, https://doi.org/10.1016/j.seppur.2019.116138.
[22] C.-X. Chen, S.-S. Yang, J. Ding, G.-Y. Wang, L. Zhong, S.-Y. Zhao, Y.-N. Zang, J.-Q. Jiang, L. Ding, Y. Zhao, L.-M. Liu, N.-Q. Ren, Non-covalent self-assembly synthesis of AQ2S@rGO nanocomposite for the degradation of sulfadiazine under solar irradiation: the indispensable effect of chloride, Appl. Catal. B: Environ. 298 (2021), 120495, https://doi.org/10.1016/j.apcatb.2021.120495.
[23] C.B. Anucha, I. Altin, E. Bacaksiz, V.N. Stathopoulos, Titanium dioxide (TiO_2)-based photocatalyst materials activity enhancement for contaminants of emerging concern (CECs) degradation: In the light of modification strategies, Chem. Eng. J. Adv. 10 (2022), 100262, https://doi.org/10.1016/j.ceja.2022.100262.
[24] C.P. Silva, D. Pereira, V. Calisto, M.A. Martins, M. Otero, V.I. Esteves, D.L.D. Lima, Biochar-TiO2 magnetic nanocomposites for photocatalytic solar-driven removal of antibiotics from aquaculture effluents, J. Environ. Manag. 294 (2021), 112937, https://doi.org/10.1016/j.jenvman.2021.112937.
[25] P.A. Pekakis, N.P. Xekoukoulotakis, D. Mantzavinos, Treatment of textile dyehouse wastewater by TiO2 photocatalysis, Water Res. 40 (2006) 1276–1286, https://doi.org/10.1016/j.watres.2006.01.019.
[26] E.S. Elmolla, M. Chaudhuri, Comparison of different advanced oxidation processes for treatment of antibiotic aqueous solution, Desalination 256 (2010) 43–47, https://doi.org/10.1016/j.desal.2010.02.019.
[27] H.E. Garrafa-Gálvez, C.G. Alvarado-Beltrán, J.L. Almaral-Sánchez, A. Hurtado-Macías, A.M. Garzon-Fontecha, P.A. Luque, A. Castro-Beltrán, Graphene role in improved solar photocatalytic performance of TiO2-RGO nanocomposite, Chem. Phys. 521 (2019) 35–43, https://doi.org/10.1016/j.chemphys.2019.01.013.
[28] D.-E. Lee, D.J. Kim, S. Moru, M.G. Kim, W.-K. Jo, S. Tonda, Highly-configured TiO2 hollow spheres adorned with N-doped carbon dots as a high-performance photocatalyst for solar-induced CO_2 reduction to methane, Appl. Surf. Sci. 563 (2021), 150292, https://doi.org/10.1016/j.apsusc.2021.150292.
[29] H. Aliyeva, A. Gurel, S. Nowak, S. Lau, P. Decorse, S. Chaguetmi, D. Schaming, S. Ammar, Photo-anodes based on TiO2 and carbon dots for photo-electrocatalytical measurements, Mater. Lett. 250 (2019) 119–122, https://doi.org/10.1016/j.matlet.2019.02.131.
[30] M. Nasirian, Y.P. Lin, C.F. Bustillo-Lecompte, M. Mehrvar, Enhancement of photocatalytic activity of titanium dioxide using non-metal doping methods under visible light: a review, Int. J. Environ. Sci. Technol. 15 (2018) 2009–2032, https://doi.org/10.1007/s13762-017-1618-2.
[31] R.M.S. Sendão, J.C.G. Esteves da Silva, L. Pinto da Silva, Photocatalytic removal of pharmaceutical water pollutants by TiO2 – carbon dots nanocomposites: a review, Chemosphere 301 (2022), 134731, https://doi.org/10.1016/j.chemosphere.2022.134731.
[32] H. Yu, R. Shi, Y. Zhao, G.I.N. Waterhouse, L.-Z. Wu, C.-H. Tung, T. Zhang, Smart utilization of carbon dots in semiconductor photocatalysis, Adv. Mater. 28 (2016) 9454–9477, https://doi.org/10.1002/adma.201602581.
[33] H. Wu, H. Xu, Y. Shi, T. Yuan, T. Meng, Y. Zhang, W. Xie, X. Li, Y. Li, L. Fan, Recent advance in carbon dots: from properties to applications, Chin. J. Chem. 39 (2021) 1364–1388, https://doi.org/10.1002/cjoc.202000609.
[34] P. Chen, F. Wang, Z.-F. Chen, Q. Zhang, Y. Su, L. Shen, K. Yao, Y. Liu, Z. Cai, W. Lv, G. Liu, Study on the photocatalytic mechanism and detoxicity of gemfibrozil by a sunlight-driven TiO2/carbon dots photocatalyst: the significant roles of reactive oxygen species, Appl. Catal. B: Environ. 204 (2017) 250–259, https://doi.org/10.1016/j.apcatb.2016.11.040.
[35] S. Sharma, A. Umar, S.K. Mehta, A.O. Ibhadon, S.K. Kansal, Solar light driven photocatalytic degradation of levofloxacin using TiO2/carbon-dot nanocomposites, N. J. Chem. 42 (2018) 7445–7456, https://doi.org/10.1039/C7NJ05118B.
[36] Y. Zeng, D. Chen, T. Chen, M. Cai, Q. Zhang, Z. Xie, R. Li, Z. Xiao, G. Liu, W. Lv, Study on heterogeneous photocatalytic ozonation degradation of ciprofloxacin by TiO2/carbon dots: kinetic, mechanism and pathway investigation, Chemosphere 227 (2019) 198–206, https://doi.org/10.1016/j.chemosphere.2019.04.039.
[37] K. Wang, L. Liang, Y. Zheng, H. Li, X. Niu, D. Zhang, H. Fan, Visible light-driven photocatalytic degradation of organic pollutants via carbon quantum dots/TiO2, N. J. Chem. 45 (2021) 16168–16178, https://doi.org/10.1039/D1NJ02387J.
[38] V.L. Louros, L.M. Ferreira, V.G. Silva, C.P. Silva, M.A. Martins, M. Otero, V. I. Esteves, D.L.D. Lima, Photodegradation of aquaculture antibiotics using carbon dots-tio2 nanocomposites, Toxics 9 (2021), https://doi.org/10.3390/toxics9120330.
[39] V. Silva, I. Invêncio, C.P. Silva, M. Otero, D.L.D. Lima, Photodegradation of oxolinic acid in aquaculture effluents under solar irradiation: is it possible to enhance efficiency by the use of TiO2/carbon quantum dots composites, Chemosphere 308 (2022), 136522, https://doi.org/10.1016/j.chemosphere.2022.136522.
[40] B. Vercelli, R. Donnini, F. Ghezzi, A. Sansonetti, U. Giovanella, B. La Ferla, Nitrogen-doped carbon quantum dots obtained hydrothermally from citric acid and urea: the role of the specific nitrogen centers in their electrochemical and optical responses, Electrochim. Acta 387 (2021), 138557, https://doi.org/10.1016/j.electacta.2021.138557.
[41] Z. Ma, H. Ming, H. Huang, Y. Liu, Z. Kang, One-step ultrasonic synthesis of fluorescent N-doped carbon dots from glucose and their visible-light sensitive photocatalytic ability, N. J. Chem. 36 (2012) 861–864, https://doi.org/10.1039/C2NJ20942J.
[42] P. Ayala, R. Arenal, A. Loiseau, A. Rubio, T. Pichler, The physical and chemical properties of heteronanotubes, Rev. Mod. Phys. 82 (2010) 1843–1885, https://doi.org/10.1103/RevModPhys.82.1843.
[43] H.M. Jeong, J.W. Lee, W.H. Shin, Y.J. Choi, H.J. Shin, J.K. Kang, J.W. Choi, Nitrogen-doped graphene for high-performance ultracapacitors and the importance of nitrogen-doped sites at basal planes, Nano Lett. 11 (2011) 2472–2477, https://doi.org/10.1021/nl2009058.
[44] S. Yu, W. Zheng, C. Wang, Q. Jiang, Nitrogen/boron doping position dependence of the electronic properties of a triangular graphene, ACS Nano 4 (2010) 7619–7629, https://doi.org/10.1021/nn102369r.
[45] V.L. dos Louros, C.P. Silva, H. Nadais, M. Otero, V.I. Esteves, D.L.D. Lima, Oxolinic acid in aquaculture waters: Can natural attenuation through photodegradation decrease its concentration, Sci. Total Environ. 749 (2020), 141661, https://doi.org/10.1016/j.scitotenv.2020.141661.
[46] D. Hazarika, N. Karak, Photocatalytic degradation of organic contaminants under solar light using carbon dot/titanium dioxide nanohybrid, obtained through a facile approach, Appl. Surf. Sci. 376 (2016) 276–285, https://doi.org/10.1016/j.apsusc.2016.03.165.
[47] K. Woan, G. Pyrgiotakis, W. Sigmund, Photocatalytic carbon-nanotube-TiO_2 composites, Adv. Mater. 21 (2009) 2233–2239, https://doi.org/10.1002/adma.200802738.
[48] F. Qin, L. Zhang, L. Tong, K. Zhang, W. Nan, J. Wang, M. Li, Photochemical transformation of sulfadiazine in UV/Fe(II)/sodium citrate Fenton-like system, J. Environ. Manag. 322 (2022), 116112, https://doi.org/10.1016/j.jenvman.2022.116112.
[49] C.-C. Yang, C.-L. Huang, T.-C. Cheng, H.-T. Lai, Inhibitory effect of salinity on the photocatalytic degradation of three sulfonamide antibiotics, Int. Biodeterior. Biodegrad. 102 (2015) 116–125, https://doi.org/10.1016/j.ibiod.2015.01.015.
[50] J. Duan, H. Jian, Q. Dou, X. Shi, R. Su, Indirect photodegradation of sulfisoxazole: effects of environmental factors (CDOM, pH, salinity, HCO3−, metal ions, halogen ions and NO3−, Mar. Pollut. Bull. 174 (2022), 113320 https://doi.org/10.1016/j.marpolbul.2022.113320.
[51] E. Evgenidou, Z. Chatzisalata, A. Tsevis, K. Bourikas, P. Torounidou, D. Sergelidis, A. Koltsakidou, D.A. Lambropoulou, Photocatalytic degradation of a mixture of eight antibiotics using Cu-modified TiO2photocatalysts: kinetics, mineralization, antimicrobial activity elimination and disinfection, J. Environ. Chem. Eng. 9 (2021), https://doi.org/10.1016/j.jece.2021.105295.
[52] A. Kutuzova, T. Dontsova, W. Kwapinski, Application of TiO2-based photocatalysts to antibiotics degradation: cases of sulfamethoxazole, trimethoprim and ciprofloxacin, Catalysts 11 (2021) 728, https://doi.org/10.3390/catal11060728.
[53] N. Malesic-Eleftheriadou, E.N Evgenidou, G.Z. Kyzas, D.N. Bikiaris, D. A. Lambropoulou, Removal of antibiotics in aqueous media by using new synthesized bio-based poly(ethylene terephthalate)-TiO2 photocatalysts, Chemosphere 234 (2019) 746–755, https://doi.org/10.1016/j.chemosphere.2019.05.239.
[54] O. Porcar-Santos, A. Cruz-Alcalde, N. López-Vinent, D. Zanganas, C. Sans, Photocatalytic degradation of sulfamethoxazole using TiO2 in simulated seawater: evidence for direct formation of reactive halogen species and halogenated by-products, Sci. Total Environ. 736 (2020), 139605, https://doi.org/10.1016/j.scitotenv.2020.139605.
[55] C. Sirtori, A. Agüera, W. Gernjak, S. Malato, Effect of water-matrix composition on Trimethoprim solar photodegradation kinetics and pathways, Water Res. 44 (2010) 2735–2744, https://doi.org/10.1016/j.watres.2010.02.006.
[56] B. Mathon, M. Ferreol, M. Coquery, J.-M. Choubert, J.-M. Chovelon, C. Miège, Direct photodegradation of 36 organic micropollutants under simulated solar radiation: comparison with free-water surface constructed wetland and influence of chemical structure, J. Hazard. Mater. 407 (2021), 124801, https://doi.org/10.1016/j.jhazmat.2020.124801.
[57] E. Felis, M. Buta-Hubeny, W. Zieliński, J. Hubeny, M. Harnisz, S. Bajkacz, E. Korzeniewska, Solar-light driven photodegradation of antimicrobials, their transformation by-products and antibiotic resistance determinants in treated wastewater, Sci. Total Environ. 836 (2022), 155447, https://doi.org/10.1016/j.scitotenv.2022.155447.
[58] S. Sanguanpak, W. Shongkittikul, C. Saengam, W. Chiemchaisri, C. Chiemchaisri, TiO2-immobilized porous geopolymer composite membrane for removal of antibiotics in hospital wastewater, Chemosphere 307 (2022), 135760, https://doi.org/10.1016/j.chemosphere.2022.135760.
[59] S. Fernandes, J.C.G. Esteves da Silva, L. Pinto da Silva, Comparative life cycle assessment of high-yield synthesis routes for carbon dots, NanoImpact 23 (2021), 100332, https://doi.org/10.1016/j.impact.2021.100332.